Journal of Hazardous Materials 180 (2010) 683–692

Contents lists available at ScienceDirect

Journal of Hazardous Materials

journal homepage: www.elsevier.com/locate/jhazmat

Amazon kaolinite functionalized with diethylenetriamine moieties for U(VI) removal: Thermodynamic of cation-basic interactions

Denis L. Guerra[a,*], Victor L. Leidens[a], Rúbia R. Viana[a], Claudio Airoldi[b]

[a] Universidade Federal de Mato Grosso, UFMT, Centro de Recursos Minerais, Cuiabá, Mato Grosso, 78060 900, Brazil
[b] Chemistry Institute, State University of Campinas, P.O. Box 6154, 13084-971 Campinas, São Paulo, Brazil

ARTICLE INFO

Article history:
Received 17 November 2009
Received in revised form 6 April 2010
Accepted 21 April 2010
Available online 29 April 2010

Keywords:
Kaolinite
Uranyl
Adsorption
Calorimetry
Thermodynamic

ABSTRACT

The compound N-[3-(trimethoxysilyl)propyl]diethylenetriamine (MPDET) was anchored onto Amazon kaolinite surface (KLT) by heterogeneous route. The modified and natural kaolinite clay samples were characterized by transmission electron microscopy (TEM), scanning electron microscopic (SEM), N_2 adsorption, powder X-ray diffraction, thermal analysis, ion exchange capacities, and nuclear magnetic nuclei of ^{29}Si and ^{13}C. The well-defined peaks obtained in the ^{13}C NMR spectrum in the 5.0–62.1 ppm region confirmed the attachment of organic functional groups as pendant chains bonded into the porous clay. The adsorption of uranyl on natural (KLT) and modified (KLT_{MPDET}) kaolinite clays was investigated as a function of the solution pH, metal concentration, temperature, and ionic strength. The ability of these materials to remove U(VI) from aqueous solution was followed by a series of adsorption isotherms adjusted to a Sips equation at room temperature and pH 4.0. The maximum number of moles adsorbed was determined to be 8.37×10^{-3} and 13.87×10^{-3} mmol g^{-1} for KLT and KLT_{MPDET} at 298 K, respectively. The energetic effects ($\Delta_{int}H$, $\Delta_{int}G$, and $\Delta_{int}S$) caused by metal cations adsorption were determined through calorimetric titrations.

© 2010 Published by Elsevier B.V.

1. Introduction

Toxic/heavy metal ions removal process involving wastewater systems is a subject of concern in view of environmental pollution control problems [1]. The presence of the radionuclides in quantities above their natural abundances in the lithosphere, even as trace amounts in the environment, is usually associated with affects the anthropogenic activity in a given ecosystem. When toxic metals are present in the aquatic system, the abatement of the pollutant to an acceptable level is necessary [2]. Uranyl is one of the contaminants found in the environment which is notoriously toxic to man and other living organisms [3]. The physicochemical behavior of uranyl in porous media and mine waste aquifers is mainly dominated by sorption and desorption reaction with solid with high porosity, particularly in the surface of clay minerals [4,5].

An especially interesting area is the control of toxic/heavy metal ions in soils and aqueous systems [6,7]. Adsorption and ion exchange processes are the most useful methods to remove them, by exploring the availability of different kinds of adsorbents associated with convenient procedures to obtained high efficiency [8]. Certain factors influence the amount of metal ions being adsorbed by mineral substrates; pH, nature of the adsorbent, adsorbent dose, initial metal ion concentration, ionic strength, and presence of competing ions. A potential important adsorbent of uranyl is layered silicates, such as kaolinite [9,10]. Kaolinite is an important phyllosilicate with flake type morphology in industrial applications due to its relevant physical and chemical properties [11]. In the last decades, kaolinite clay has been investigated as an adsorbent in the removal of organic contaminants and heavy metal ions from aqueous medium in the natural environmental [12]. Kaolinite clay is a significant component of many soils of tropical regions. There are large reserves of kaolinite in north Brazil, Amazon region. The specific physical–chemical properties and large distribution of kaolinite make it to be studied and used extensively as adsorbent [9].

Porous organic–inorganic hybrid materials have attracted considerable attention, layer silicate nanolayers can be utilized as alternative inorganic agent for the composition of nanostructured organic–inorganic hybrids composites [13–15]. A large number of different adsorbent materials containing a variety of attached chemical functional groups has been reported for this purpose. In recent years, special attention has been focused on the use of natural clay adsorbents as an alternative to replace the conventional adsorbents. Covalent immobilization onto layer silicate supports of a desired chelate moiety, with the specific purpose of obtaining selective adsorbent materials is one of the most important procedures to develop highly selective matrices. Designed applications to improve environmental quality through radionuclide removal

* Corresponding author. Tel.: +55 19 33429407; fax: +55 19 33429407.
E-mail addresses: denis@cpd.ufmt.br, dlguerra@pq.cnpq.br (D.L. Guerra).

0304-3894/$ – see front matter © 2010 Published by Elsevier B.V.
doi:10.1016/j.jhazmat.2010.04.092

have recently been emerged. Moreover, the versatility of the kaolinite clay support to be chemically modified induces its application to produce new materials available to remove contaminates from water and soils [9,16].

This investigation reports the use of original and modified kaolinite samples as alternative absorbents for extraction of toxic metals, which are commonly present in waters from a variety of sources and industrial effluents. For this propose, the adsorption isotherms of U(VI) from aqueous medium at room temperature were explored, bearing in mind the influence of different parameters such as solution pH, metal concentration, temperature, and ionic strength. Amazon kaolinite clay sample has been chemically modified with (MPDET) using the heterogeneous route. From calorimetric measurements involving such heterogeneous system, the quantitative nitrogen/cation interaction at the solid/liquid interface was determined.

2. Experimental section

2.1. Raw material and reagents

The clay sample used in this investigation was obtained from the Tabatinga area, Amazonas state, North of Brazil, Amazon region. A natural kaolinite sample, named KLT, with less than 2 μm particles, was separated by sedimentation. The clay sample was activated in a stream of dry hydrogen by heating at 423 ± 1 K for 12 h and used immediately.

The reagents, N-[3-(trimethoxysilyl)propyl]diethylenetriamine (MPDET) $(CH_3O)_3Si(CH_2)_3(NH)_2(CH_2)_4NH_2$ and *n*-dodecylamine (DDA) $CH_3(CH_2)_{11}NH_2$, were from Aldrich and used as received. Other chemicals such as methanol and ethanol were of reagent grade. Doubly distilled deionized water (DDW) was used for the preparation of solutions, wherever required. Solutions of uranyl were prepared from suitable reagent grade nitrate salt by dissolving in DDW.

2.2. Organofunctionalization of kaolinite clay

The functionalized hybrid material was synthesized by maintaining the reagent molar ratios as 1:200:50:0.3, respectively, for *n*-dodecylamine, deionized water, ethanol, and silylating agent [13,14]. In the first step, *n*-dodecylamine was mixed with deionized water and ethanol and allowed to stir continuously for 45 min. In the second step, approximately 5 g of kaolinite clay sample were added to the mixture and the stirring was continued for 50 min. During this time period the silylating agent (MPDET) was added drop-wise to form the final hybrid material, which is called KLT_{MPDET}. After addition of silylating agent, the resulting mixture was further stirred for 20 h at 291 ± 1 K. At the end of the above process, the material was centrifuged, washed with deionized water and air dried at room temperature for 30 h. The final material was subjected to Soxhlet extraction for 72 h using ethanol as solvent [13,14].

2.3. Characterization methods

Transmission electron microscopy (TEM) image was recorded on a JEM 3010 URP microscope at LNLS/Brazil with an accelerating voltage of 300 kV. For this determination the sample was prepared by placing a drop of a suspension of particles dispersed in isopropanol onto a carbon-coated copper grid.

The natural and modified kaolinite clays were analyzed by scanning electron microscopy (SEM) in JEOL microscope, model JEOL JSM 6360LV, using an acceleration voltage of 15 kV and magnification ranging from 300 to 3000 fold.

Nuclear magnetic resonance spectra of the samples were obtained on a Brucker AC 300/P spectrometer at room temperature. For each run, approximately one gram of each solid sample was compacted into a 7 mm zirconium oxide rotor. The measurements were obtained at frequencies of 59.63 and 75.47 MHz, for silicon and carbon atoms, respectively, with a magic angle spinning of 4 kHz. In order to increase the signal to noise ratio of the solid-state spectra, the CP/MAS technique was used. ^{29}Si and ^{13}C CP/MAS spectra were obtained with pulse repetitions of 3 s for both nuclei and contact times of 1 and 3 ms, respectively.

The natural kaolinite clay was analyzed by inductively couple plasma optical emission spectrometry (ICP OES) using a Perkin Elmer 3000 DV instrument.

X-ray powder diffraction (XRD) patterns were recorded with Philips PW 1050 diffactometer using CuKα (0.154 nm) radiation in the region in the between 2° and 65° (2θ) at a speed of 2°/min and in steps of 0.050°.

Brunauer–Emmett–Teller (BET) surface area, pore diameter and pore volume were obtained from nitrogen adsorption/desorption in a Micromeritics ASAP 2000 BET surface analyzer system. The mesopore size distribution was obtained by applying the Barret–Joyner–Halenda (BJH) method to the adsorption branch of the isotherm.

The cation exchange capacities (CEC) of natural and modified kaolinites clay samples were followed by the ammonium acetate method with a concentration of 2.0 mol dm^{-3} at pH 8.0.

Thermogravimetric curves were recorded using DuPont model 1090 B apparatus coupled to a model 951 thermobalance, on heating from room temperature to 1273 ± K at a heating rate of 0.17 K s^{-1} in an argon flow of 1.67 cm^3 s^{-1}. The samples varied in weight from 15.0 to 30.0 mg.

2.4. Batch adsorption study

The adsorption experiments were performed through the batch-wise method by suspending a series of 20 mg samples of the solid, in 20.0 cm^3 aqueous solutions of cations at concentrations varying from 1.25×10^{-2} to 3.00×10^{-1} mmol dm^{-3}, under orbital stirring for 24 h at 298 ± 1 K [16,17]. Profiles of the obtained adsorption isotherms were represented by the number of moles adsorbed (N_f), versus the number of moles at equilibrium per volume of solution (C_S), for series of isotherms, the data reveal that the adsorption process conforms to the Sips model (Eq. (1)) [18].

$$N_f = \frac{N_S K_S C_S^{\frac{1}{n}}}{1 + K_S C_S^{\frac{1}{n}}} \quad (1)$$

where C_s is the concentration of the solution at equilibrium (mol dm^{-3}), N_f the number of moles of metal cation adsorbed per gram of the phyllosilicate in each adsorption obtained by batch procedure, N_S the amount of cation necessary for the formation of the monolayer, which depends on the number of available adsorption reactive sites, K_S is the equilibrium constant and n is the Freundlich exponent. The effect of pH on adsorption for all clay samples was evaluated by varying this parameter over the range from 1.0 to 5.0, with addition of 0.10 mol dm^{-3} of nitric acid or sodium hydroxide. The pH of the solutions was measured using a pH/Ion Analyzer, model 450 M.

Uranyl concentrations in the supernatant were determined using the kinetic phosphorescence analyzer KPA-10. The uranyl samples and reference are excited by firing the nitrogen laser at 337 nm. This excites the dye laser to produce an excitation wavelength of 420 nm. Each analysis is a repetition of 50 cycles. A 3 ns laser pulse initiates each cycle. For each experiment pint, the reproducibility was checked by at least duplicate run.

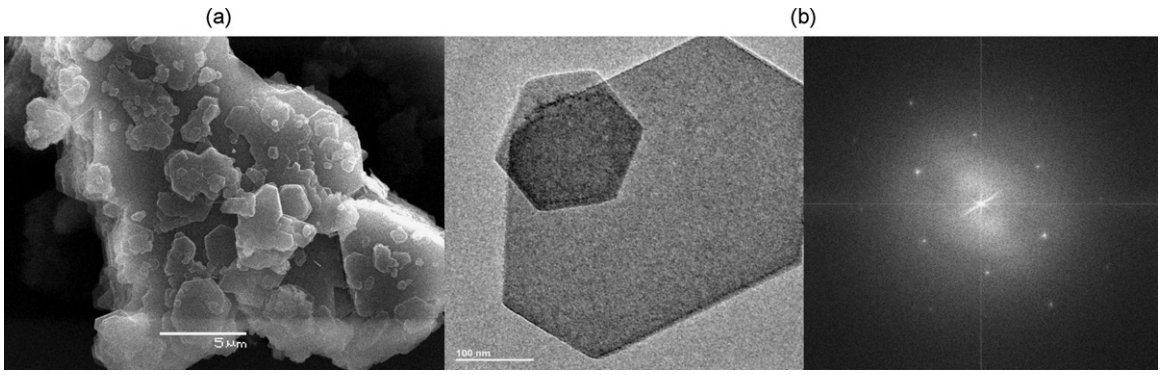

Fig. 1. Morphology of the natural kaolinite sample: SEM (a) and TEM (b).

2.5. Thermodynamic

The thermal effects from metal cation interacting on natural and modified kaolinite samples were followed by calorimetric titrations using an isothermal calorimeter, Model LKB 2277, from thermometric. In this titration, the metallic solution is added to a suspension of about 20 mg of the phyllosilicate sample in 2.0 cm^3 of water, under stirring at 298 ± 1 K. A series of increments of 10 μL of metal solutions was added to the metal-silicate to obtain the thermal effect of interaction (Q_t). Two other titrations are needed to complete the full experiment: (i) the thermal effect due to hydration of the silicate sample (Q_h), which normally gives a null value and (ii) and the dilution effect of metal solution in water, without sample in the vessel (Q_d). The resulting thermal effect is given by following equation: $\Sigma Q_r = \Sigma Q_t - \Sigma Q_d$ [19]. The molar enthalpy ($\Delta_{int}H$) of the interaction process can be calculated by the expression $\Delta_{int}H = \Delta_{int}hN_S$, were $\Delta_{int}h$ is enthalpy of interaction to form a monolayer per unit mass of matrices. The Gibbs free energy can be calculated by the equation $\Delta_{int}G = RT \ln K_S$ equation, the entropy is finally calculated from $\Delta_{int}G = \Delta_{int}H - T\Delta_{int}S$ [20].

2.6. Parameter optimization with FITEQL

The computer code FITEQL is a program for determining chemical equilibrium constants from experimental data. In the present context, the input data for FITEQL are the experimental data for U(VI) adsorption as a function of pH. The Davis equation [21] was used for activity correction. Relative errors of 1% in the concentration of surface sites, total U(VI), and adsorbent U(VI), and relative errors of 4% in log [H^+] and log [H_2CO_2] were used as FITEQL input values [22].

3. Results and discussion

3.1. Characterization of materials

Morphology as well as structural ordering of the natural kaolinite, presented in Fig. 1a and b, was analyzed by SEM and TEM. The individual crystals presented themselves as flakes in a pseudo-hexagonal morphology, as confirmed by TEM images. The presence of agglomerated particles of nanodimensions was also noted in the natural kaolinite sample. Also twinned of edges and well-defined angles were observed. Small aggregates of rounded crystal coexisted with hexagonal kaolinite particles with particle size mostly smaller than 5.0 μm as illustrated in Fig. 1b. This morphology was similar to that described by Keller [23] for weathered hydrothermal kaolin samples, with particles and 'books' randomly oriented. In general, kaolinite crystals of large size (>1.0 μm) showed pseudohexagonal form and well-defined edges, whereas the edges of crystals of small sizes were rounded.

Nuclear magnetic resonance in the solid-state is a technique to give valuable information about the bonding of the pendant chains anchored on an inorganic backbone. For this purpose silicon and carbon nuclei were examined in order to better characterize the natural and modified kaolinite clays. The ^{29}Si NMR spectra

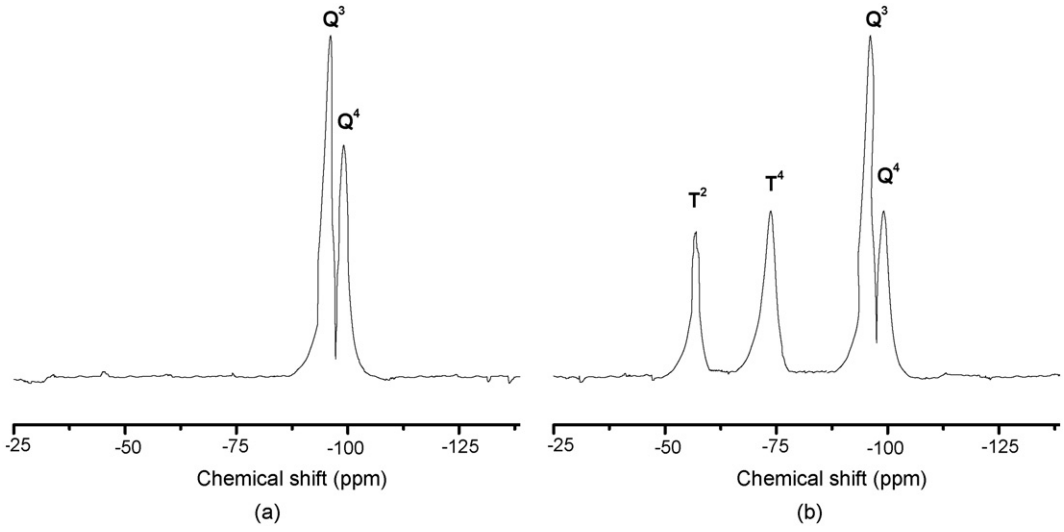

Fig. 2. ^{29}Si MAS NMR spectra of unmodified and modified kaolinite samples: KLT (a) and KLT_{MPDET} (b).

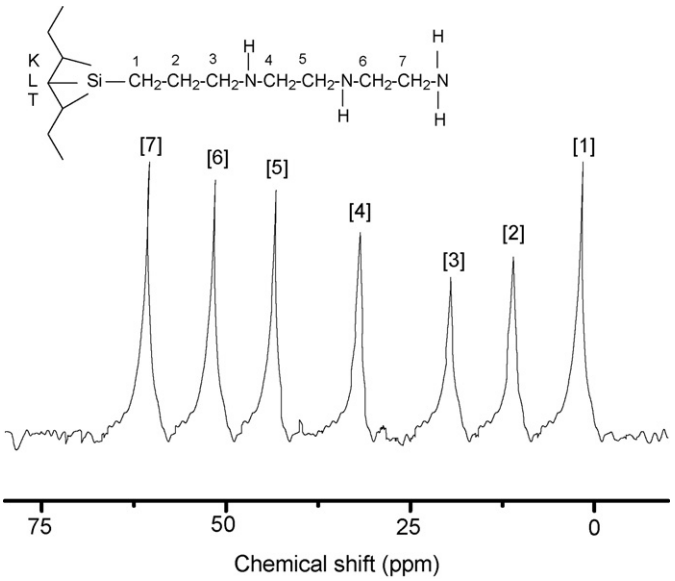

Fig. 3. ^{13}C MAS NMR spectrum of modified kaolinite sample, KLT_{MPDET}.

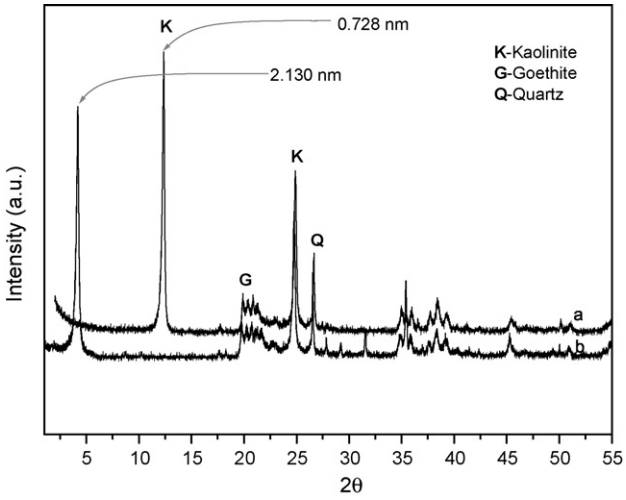

Fig. 4. X-ray diffraction patterns for unmodified and modified kaolinite samples: KLT (a) and KLT_{MPDET} (b).

of the natural and modified kaolinite clays, presented in Fig. 2a and b, respectively, shows a series of typical phyllosilicate signals that correspond to (i) $Si(OSi)_4$, Q^4, at 102.0 ppm, (ii) $Si(OSi)_3OH$, Q^3, at −92.0 ppm while (iii) a possible weak broad shoulder at −91.0 ppm could be assigned to Q^2, $Si(OSi)_2(OH)_2$. Two other peaks found at −72.0 and −58.0 ppm were assigned to $RSi(OSi)_3$ (T^3) and $RSi(OSi)(OH)_2$ (T^2) signals, respectively. These signals originate from the structural units related to the presence of an organic part covalently bonded to the inorganic backbone silicate structure. The relative intensity of the peak for Q^3 was higher in comparison to Q^4 species and this is in agreement with similar observations in the case of hybrid materials. The covalent silylating agent attachment as tripoid bonding on inorganic structure is confirmed by the presence of T^3 species, which assigned sequence of organic carbon atoms chain, without any template agent, is supported by ^{13}C NMR [25,26].

The hybrid material showed well-resolved peaks positioned at 5.0, 13.0, and 20.0 ppm for the spacer propyl chain carbon atoms attached to phyllosilicate. Other carbon atoms, numbered as in the proposed structure, were observed at 37.0 and 46.0 ppm, respectively, assigned to C_4 and C_5, and other peaks at 58.0 and 62.1 ppm were assigned to C_6 and C_7, respectively, as illustrated in Fig. 3. All the assignments were in good agreement with previously studied systems. Thus, the sequence of peaks presented in the spectrum for the hybrid materials confirms the sequence of carbons of the pendant groups obtained by the synthetic method employed in the synthesis of these kinds of hybrids materials [26].

Elemental analyzes from the ICP OES technique for the original clay sample, KLT, gave results consistent with kaolinite with silicon and aluminum being the major components. The total mineralogical composition is given by 46.26%; 39.62%; 0.47%; 0.28%; 0.27%; 0.21% and 0.17% of SiO_2, Al_2O_3, Fe_2O_3, MgO, Na_2O, CaO, and K_2O respectively, and 12.73% of mass was lost in the ignition process. The composition of the original kaolinite sample was calculated through the chemical analysis, to give the formula (Eq. (2)):

$$(Al_{1.28}Fe_{0.24}Mg_{0.13}Na_{0.12}Ca_{0.10}K_{0.09})(Si_2O_5)(OH)_4 \quad (2)$$

The X-ray diffraction patterns for samples showed at low angle the characteristic reflection related to the kaolinite clay samples [9]. The determination of the total mineralogical composition of the pristine natural clay sample was carried out on oriented mounts, exhibiting mainly kaolinite, quartz, and goethite, as shown in Fig. 4. After intercalation process the kaolinite presented, as expected, an increase in basal distance, changing the d_{001} value from 0.728 nm for natural kaolinite to 2.130 nm for the intercalated form (Fig. 4a and b). It was also observed that the KLT sample presents a slightly broader and less intense peak, in comparison with KLT_{MPDET}, a behavior that could be attributed to differences in the degree of crystallinity [9]. This fact confirms that the organic(inorganic precursor was successfully intercalated into the interlayer space with the MPDET units perpendicularly oriented to the phyllosilicate layer. The great influence of the number of MPDET ions on the sur-

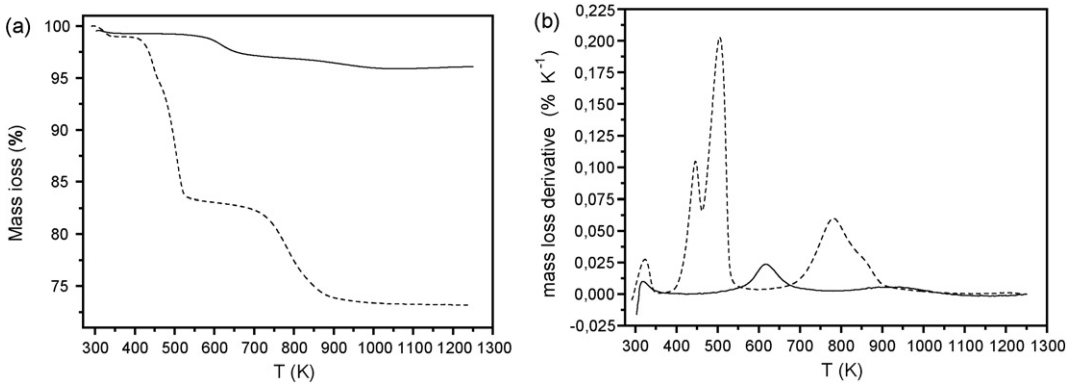

Fig. 5. Thermogravimetric (a) and derivative (b) curves for KLT (–) and KLT_{MPDET} (. . .).

Table 1
Textural properties and cation exchange capacity (CEC) of natural and modified kaolinite samples.

Sample	Surface area-SA_{BET} ($m^2\ g^{-1}$)	Micropore area ($m^2\ g^{-1}$)	Average pore diameter (nm)	Pore volume ($cm^3\ g^{-1}$)	CEC (meq/100 g of clay)
KLT	35.0	10.0	1.1	0.08	15.0
KLT_{MPDET}	889.7	38.1	4.8	0.30	138.5

face and on the constitution and distribution of the ions has been previously reported [13,14].

The Thermogravimetric and the corresponding derivative curves are shown in Fig. 5a and b, respectively. The original kaolinite sample presented mass loss in only one step from 300 to 500 K, as clearly indicated by the derivative curve, showing only one simple peak. However, a small mass loss at a lower temperature, related to humidity, gave a small peak at 340 K, also indicated in the corresponding derivative curve. Identically, functionalized kaolinite sample presented at low temperature from 300 to 370 K, a mass loss which could be attributed of ethanolic molecules desorption. From this stage three other mass losses in the 400–470 K; 470–600 K and 600–950 K intervals are observed, which are confirmed by the set of three peaks in the derivative curve (Fig. 6b). The first stage can be attributed to hydrating water, whereas the second step is due to dehydroxylation partial of the silicate structure. The peak in the 600–950 K interval can be attributed to decomposition of functionalized species, MPDET ions.

The BET surface areas of the natural and modified clay samples demonstrated that chemical modification caused the formation of micropores in the solid particles, resulting in a higher surface area, revealing 889.7 $m^2\ g^{-1}$ for KLT_{MPDET} and relative to the natural KLT sample with 35.0 $m^2\ g^{-1}$. The pore diameters change in the same direction, varying from 1.4 nm for the natural to 4.8 nm for the anchored clay. The textural properties of natural and modified kaolinite samples are reported in Table 1, which depends on particle size shape, and distribution of cracks and pores in the material, and therefore, cannot be represented as a general characteristic of particular type of material.

The cation exchange capacity of clay mineral is attributed to structural defects, broken bonds and structural hydroxyl transfers [12], which are obviously in short supply in kaolinite (structure 1:1-TO) than in montmorillonite (structure 2:1-TOT). Intercalation process increases the total number of exchange sites marginally in kaolinite. The CEC of natural kaolinite was found to be 15.0 meq/100 g of clay, and modified kaolinite was found to be 138.5 meq/100 g of clay, as listed in Table 1. These results are in accordance with finding from Unuabonah et al. [27], who found that the intercalation of sulphate and tripolyphosphate (TPP) in kaolinite (Delta State, Nigeria) tended to be more successful by impregnation method.

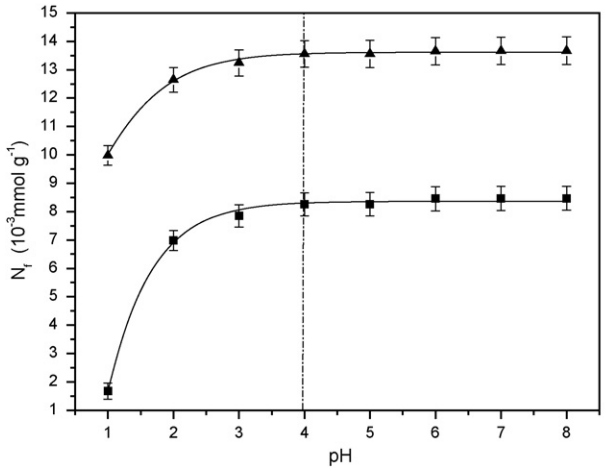

Fig. 6. Effect of pH on cations adsorption onto unmodified and modified kaolinite samples from aqueous solution: KLT (■) and KLT_{MPDET} (▲) (clay 1.0 g dm^{-3}, time 8.0 h, and controlled temperature in 298 ± 1 K).

3.2. Effects of pH and ionic strength

The adsorption rate is influenced by many factors, including solubility and molecular size of the adsorbate, characteristics of the adsorbent, and agitation. Changes in pH of the medium are one of the most important factors affecting the concentration and metal recovery procedure, which is related to the formation of soluble metal complexes and subsequently their stabilities in aqueous solutions. It is well known that surface charge of adsorbent can be modified by changing the pH of the solution and the chemical species in the solution depends on this parameter. Fig. 6 shows the influence of pH in adsorption process of uranyl onto natural and modified matrices. The data reveals maximum values of N_f around pH 4.0 for all matrices. The adsorption of uranyl on natural and modified kaolinite clays mainly occurs at pH < 4.0. The adsorption of U(VI) increases quickly at pH < 4.0. Results emphasize that with increase in pH of solution, the N_f adsorbed increases for all systems. Therefore the efficiency of uranyl on unmodified and modified phyllosilicates can be controlled by the initial pH of the solid/liquid reaction. The reason for low adsorption capacity in high pH is the coulombic repulsion between the negative charge of adsorbent surface and the hydrolysis species of uranyl. In addition, as pH is increased there is a decrease of positive surface charge, which results in lower coulombic repulsion of the adsorbing metal ions.

According to some reports, the decrease in adsorption rate occurs because the surface of the adsorbent becomes negatively charged and coulombic repulsion is enhanced. According to Stumm and Sulzberger [28], the decrease is because of ligand exchange, were anions react with surface hydroxides on the adsorbents. While previous surface complexation modeling studies have predicted the presence of polymeric uranyl adsorbate species on lamellar phyllosilicates, such as, montmorillonite, attapulgite, and kaolinite [29,30]. Polymeric surface complexes have generally been assumed to be comprised of one of the polymeric solution species that predominate at near neutral pH values, most notably $(UO_2)_3(OH)_5^+$.

Single-species uranyl adsorption scenarios generally agreed upon are outer-sphere binding at cation exchange sites at low pH and low ionic strength, and inner-sphere binding to hydroxylated edge sites at neutral pH and high ionic strength. In Fig. 7a and b shows uranyl adsorption on the natural and modified kaolinite clays as a function of pH and U(VI) concentration. Overall fractional adsorption was insensitive to charges in the U(VI) concentration at the three lower concentrations studied (0.01×10^{-3}, 0.5×10^{-3}, and 1×10^{-3} mmol dm^{-3}). Uranyl adsorption increased with increasing pH up to approximately 8, and decreased with increasing pH from 8.0 to 10, this adsorption behavior was observed for all systems. The distinctive pH-dependent adsorption behavior is attributed to the influence of hydrolysis and carbonate complex formation on uranyl aqueous speciation. Table 2 lists the equation thermodynamic data used calculations [31,32]. The UO_2^{2+} has at least six hydrolysis species present at appreciable levels in dilute solutions in the presence of dissolved CO_2 and below pH 10.0 (i.e., UO_2^{2+}, $UO_2(OH)^+$, $UO_2(OH)_2^0$, UO_2CO_3,

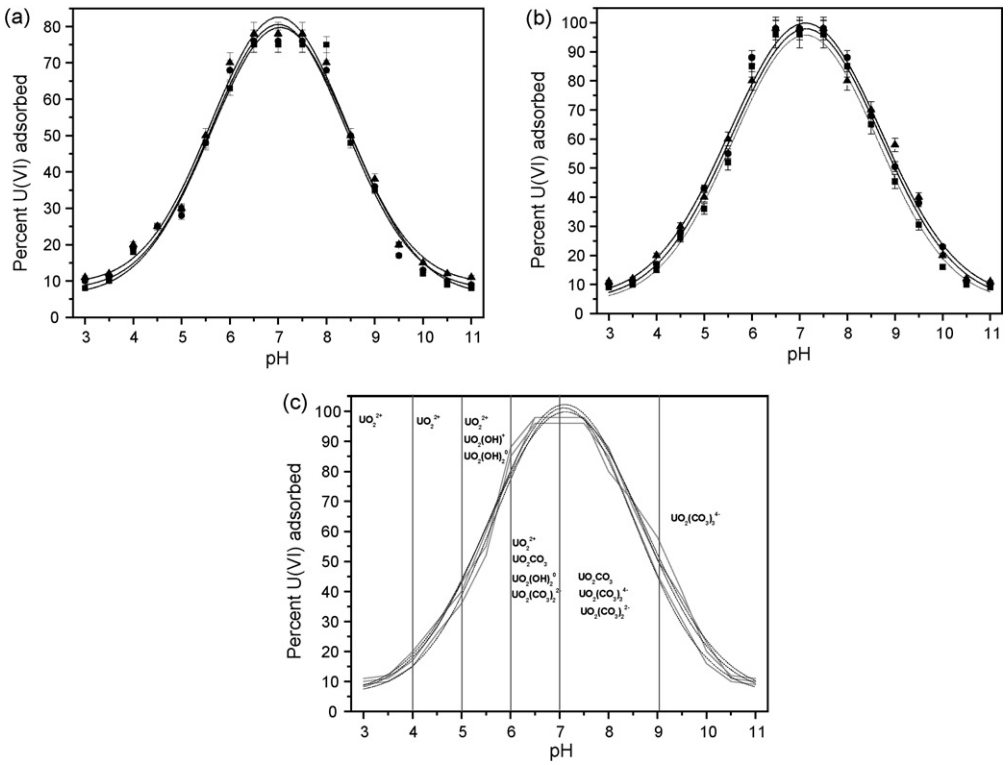

Fig. 7. Experimental and model-calculated percent uranyl adsorbed as a function of pH and U(VI) concentration on natural and modified kaolinite clays (3.0 g dm^{-3}) in 0.1 mol dm^{-3} $NaNO_3$: KLT (a) and KLT_{MPDET} (b); U(VI) concentration and $P_{CO_2} = 10^{-3.5}$ atm: 0.01×10^{-3} mmol dm^{-3} (▲), 0.5×10^{-3} mmol dm^{-3} (●), and 1×10^{-3} mmol dm^{-3} (■) and demonstrative of the relative species of U(VI) as a function of pH values (c).

$UO_2(CO_3)_2^{2-}$, and $UO_2(CO_3)_3^{4-}$). At pH < 4.0, UO_2^{2+} is the main species (99 ± 0.9%); at pH 5–6, UO_2^{2+} (68.0 ± 0.5%), $UO_2(OH)^+$ (25.0 ± 1.0%), and $UO_2(OH)_2^0$ (5.0 ± 1.0%), At pH 6.0–7.0, the predominant species are UO_2CO_3 (80.0 ± 0.5%), UO_2^{2+} (6.0 ± 0.5%), $UO_2(OH)_2^0$ (4.0 ± 1.0%), and $UO_2(CO_3)_2^{2-}$ (8.0 ± 0.5%); at pH > 7.0, the predominant species are $UO_2(CO_3)_2^{2-}$ (91 ± 1.0%), UO_2CO_3 (5 ± 0.5%), and $UO_2(CO_3)_3^{4-}$ (2 ± 1.0%), and finally at pH > 9.0, the predominant species is $UO_2(CO_3)_3^{4-}$ (99 ± 1.0%), and other species are <1.0% (Fig. 7c). Similar uranyl adsorption behavior has been reported on various lamellar phyllosilicate such as kaolinite clay, synthetic imogolite, goethite, lepidocrocite, muscovite, and mackinawite [33].

Table 2
Formation constants for aqueous solution.

Species	Reaction	Log β ($I = 0$)[a]
UO_2OH^+	$UO_2^{2+} + H_2O \Leftrightarrow UO_2OH^+ + H^+$	−5.25
$UO_2(OH)_{2aq}$	$UO_2^{2+} + 2H_2O \Leftrightarrow UO_2(OH)_{2aq} + 2H^+$	−12.15
$UO_2(OH)_3^-$	$UO_2^{2+} + 3H_2O \Leftrightarrow UO_2(OH)_3^- + 3H^+$	−20.25
$UO_2(OH)_4^{2-}$	$UO_2^{2+} + 3H_2O \Leftrightarrow UO_2(OH)_4^{2-} + 4H^+$	−32.40
$(UO_2)_2OH^{3+}$	$2UO_2^{2+} + H_2O \Leftrightarrow (UO_2)_2OH^{3+} + H^+$	−2.70
$(UO_2)_2(OH)_2^{2+}$	$2UO_2^{2+} + 2H_2O \Leftrightarrow (UO_2)_2(OH)_2^{2+} + 2H^+$	−5.62
$(UO_2)_3(OH)_4^{2+}$	$3UO_2^{2+} + 4H_2O \Leftrightarrow (UO_2)_3(OH)_4^{2+} + 4H^+$	−11.90
$(UO_2)_3(OH)_5^+$	$3UO_2^{2+} + 5H_2O \Leftrightarrow (UO_2)_3(OH)_5^+ + 5H^+$	−15.55
$(UO_2)_3(OH)_7^-$	$3UO_2^{2+} + 7H_2O \Leftrightarrow (UO_2)_3(OH)_7^- + 7H^+$	−32.20
$(UO_2)_4(OH)_7^+$	$4UO_2^{2+} + 7H_2O \Leftrightarrow (UO_2)_4(OH)_7^+ + 7H^+$	−21.9
UO_2CO_{3aq}	$UO_2^{2+} + CO_3^{2-} \Leftrightarrow UO_2CO_{3aq}$	9.94
$UO_2(CO_3)_2^{2-}$	$UO_2^{2+} + 2CO_3^{2-} \Leftrightarrow UO_2(CO_3)_2^{2-}$	16.61
$UO_2(CO_3)_3^{4-}$	$UO_2^{2+} + 3CO_3^{2-} \Leftrightarrow UO_2(CO_3)_3^{4-}$	21.84
$UO_2NO_3^+$	$UO_2^{2+} + NO_3^- \Leftrightarrow UO_2NO_3^+$	0.30
$UO_2SiO(OH)_3^+$	$UO_2^{2+} + Si(OH)_{4aq} \Leftrightarrow UO_2SiO(OH)_3^+ + H^+$	−1.84
HCO_3^-	$H_2CO_3 \Leftrightarrow H^+ + HCO_3^-$	−6.35
CO_3^{2-}	$H_2CO_3 \Leftrightarrow 2H^+ + CO_3^{2-}$	−16.68
$NaHCO_3^0$	$Na + HCO_3^- \Leftrightarrow NaHCO_3^0$	0.16[b]
$NaCO_3^-$	$Na + CO_3^{2-} \Leftrightarrow NaCO_3^-$	0.15[b]

[a] All UO_2^{2-} values from Guillaumont et al. [31].
[b] Values from Nakayama [32].

Similar pH-dependent uranyl adsorption is also observed at other ionic strengths (i.e., 0.02, 0.1, and 0.5 mol dm^{-3}) (Fig. 8a and b) adsorption is relatively independent to changes in ionic strength at pH < 7.5, but UO_2^{2+} adsorption decreased with increasing of sodium nitrate concentration in range from 0.2 to 0.5 mol g^{-1} in the alkaline pH range (7.0–10.0). Similar studies showed that ionic strength dependence of uranyl adsorption in the alkaline pH range can be expected because of the charge in activity of the aqueous uranyl-carbonate complexes. In addition, the dependence of adsorption on ionic strength in this pH range cannot be used to argue that outer-sphere complexes are the predominant uranyl surface species. To better understand the uranyl surface speciation at the natural- and modified kaolinites-water interface.

3.3. *Effect of concentration*

The available reactive atoms from the organic molecules, the maximum adsorption values are listed in Table 3 (%) and Table 4 (mmol g^{-1}) and the adsorption isotherms shown in Fig. 9a, suggested that only one cation can saturate these basic reactive centers introduced in kaolinite structure. Same examples of different adsorbents focusing on the available uranyl extraction data from aqueous solutions are listed in Table 3. From 12 different adsorbents presented none of them presented higher adsorption capacities than natural and modified materials for U(VI) uptake, indicating that these adsorbents could be successfully employed for removal of uranyl from aqueous solution [34–36]. As observed the present series of results obtained from unmodified and modified silicates present the same order of magnitude as those obtained with the montmorillonite SWy-2 was obtained from the Source Clay Repository of the Clay Mineral Society (CMS) (USA) [36], synthetic imogolite [$HOSiO_3Al_2(OH_3)$] [32] and kaolinite samples obtained from Washington Country, Georgia, Source Clay Repository of the

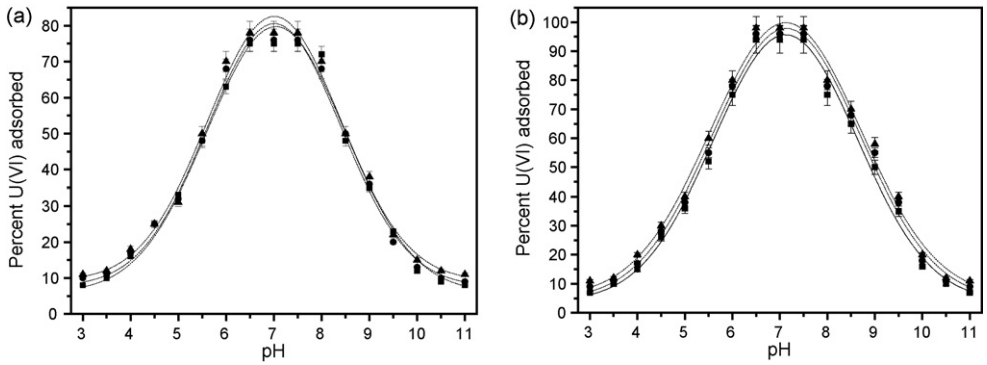

Fig. 8. Experimental and model-calculated percent uranyl adsorbed as a function of pH and ionic strength on natural and modified kaolinite clays (3.0 g dm^{-3}) in 1×10^{-3} mmol dm^{-3} U(VI) and $P_{CO_2} = 10^{-3.5}$ atm: KLT (a) and KLT_{MPDET} (b); $NaNO_3$ concentration: 0.02 mol dm^{-3} (▲), 0.1 mol dm^{-3} (●), and 0.5 mol dm^{-3} (■).

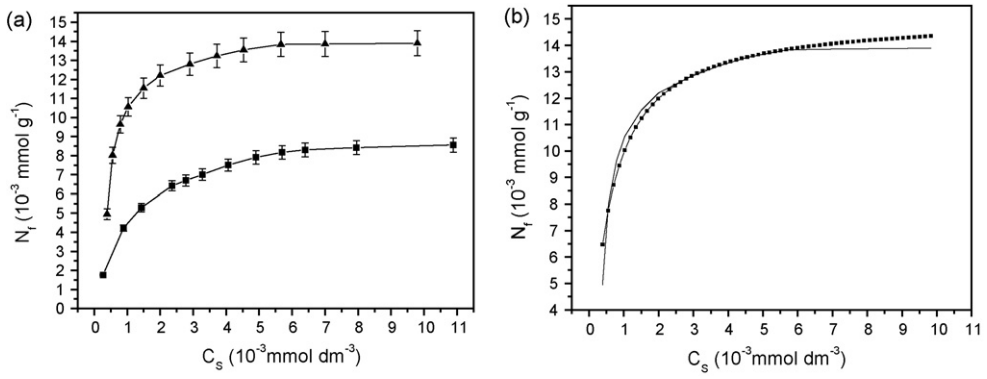

Fig. 9. Adsorption performance of natural and modified kaolinite samples in uranyl aqueous solution: KLT (■) and KLT_{MPDET} (▲) (a), experimentally adjusted data with Sips non-linear model, experimental (–) and calculated (■) curves (b) (clay 3.0 g dm^{-3}, pH 2.0, time 8.0 h, and controlled temperature is 298 ± 1 K).

Clay Mineral Society (CMS) (USA) [8], as listed in Table 3 [3,17,10,36–44].

The metal adsorptions on natural and chemically immobilized kaolinite samples are shown in Fig. 9a. The molecules anchored onto the oxides containing nitrogen basic atoms on pendant chains favor a metal interaction, mainly of soft cations, due to the presence of the basic reactive centers [45]. Based on the structural features presented by basic groups on the natural or modified clay surfaces, the adsorption can be related directly to the available nitrogen atoms.

The large capacity of modified kaolinite sample was confirmed through constant values obtained with this model in the non-linear form, whose results gave the best approximation to the experimental data, as illustrated in Fig. 9b. The values are listed in Table 4. The large capacity of adsorption of the anchored kaolinite is represented by these constant values, which can be attributed to the immobilization of reactive basic groups on the pendant chains. Thus, the attached groups are the reactive basic center that contributes directly to the adsorption property of the anchored kaolinite sample.

The kaolinite cation adsorption capacity for all these matrices depends on the nature of the complex formed on surface and also on the affinity of the metal for any particular attached ligand [46]. The maximum cation adsorption capacity, N_f^{max}, for natural and organo functionalized kaolinite clays is listed in Table 4, these values were obtained experimentally, with the highest values for the chemically modified surface, showing also an increase with variation of uranyl concentration. These N_f^{max} values reflect the good affinity of the nitrogen donor atoms attached to the inorganic backbone for bonding uranyl. Favorable nitrogen/uranyl interactions were pre-

Table 3
Comparison of the maximum adsorption capacity (N_f^{max}) of U(VI) on some natural and synthetic adsorbents from aqueous solution.

Adsorbents	N_f^{max} (mmol dm^{-3})	R_e (%)	Reference
Na-kanemite	–	97.0	[3]
Kaolinite (Georgia-USA)	–	99.0	[10]
Na-magadiite	–	96.0	[17]
Montmorillonite – SWy-2 (Clay Mineral Society)	1.96×10^{-3}	99.0	[36]
Imogolite	–	98.0	[37]
Biotites (Ontario-Canada)	2.0×10^{-1}	45.0	[38]
Analogue of heulandite	–	95.0	[39]
Attapulgite Kaixi (Gansu-China)	7.5×10^{-3}	–	[40]
Aquifer sediments (Hanford Site-Washington-USA)	1.0×10^{-3}	–	[41]
Gibbsite(Najing-China)	–	97.0	[42]
Goethite	–	98.0	[43]
Analogue of mesolite	–	65.0	[44]
KLT	–	28.9	This work
KLT_{MPDET}	–	99.0	This work

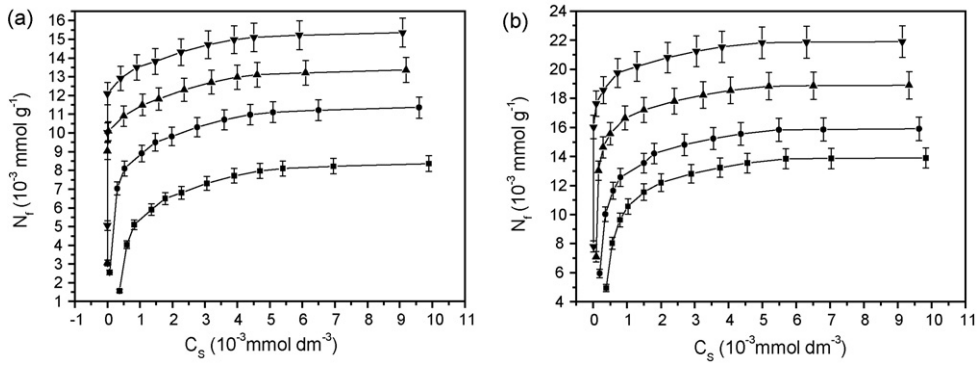

Fig. 10. Effect of temperature of adsorption U(VI) on natural and modified kaolinite clays at 298 K (■), 303 K (●), 308 K (▲) and 313 K(▼). KLT (a) and KLT_{MPDET} (b) (clay 1.0 g dm^{-3}, pH 4.0, and time 8.0 h).

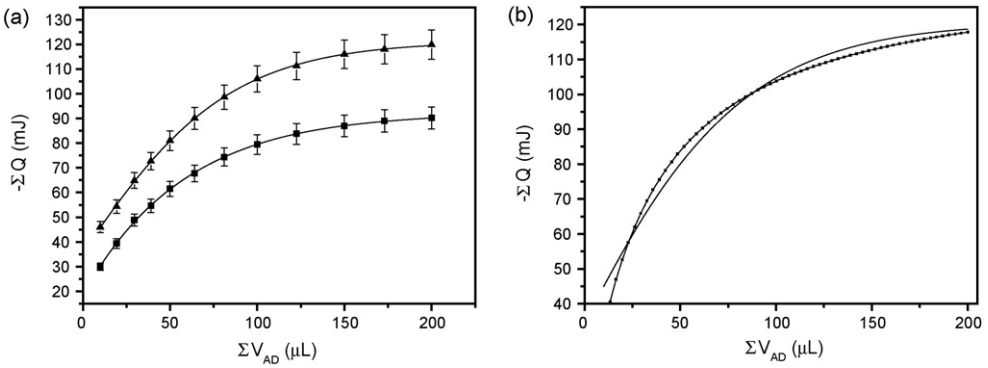

Fig. 11. The resulting thermal effects of the adsorption isotherms for the uranyl: KLT (■) and KLT_{MPDET} (▲) (a) and example of curve obtained by non-linear regression-KLT_{MPDET}/U(VI) (experimental (–) and calculated (■)) (b) (clay 1.0 g dm^{-3}, pH 4.0, and time 8.0 h).

viously observed for these silylating agents when immobilized on phyllosilicate.

3.4. Effect of temperature

Amount of radionuclide adsorbed at four different temperatures of 298, 303, 308, and 313 K showed an increasing trend with increase in temperature. Typical results are shown in Fig. 10a and b and Table 4 with the highest pronounced adsorption for modified kaolinite in 313 K. It is likely that adsorption of radionuclide on kaolinite clay surfaces requires activation energy and rise in temperature helps more radionuclide ion to overcome this energy barrier and get attached to the clay surfaces. Another possibility is the creation of additional adsorption reactive sites on kaolinite surfaces arising due dissociation of some of the surface components of natural and modified kaolinite samples at a temperature higher than the ambient which increase radionuclide uptake. These influences may operate independently of one another or may be operational simultaneously in reactive clay surfaces.

3.5. Thermodynamic study

From calorimetric titration data, the net thermal effects resulted in the corresponding well-behaved isotherms that were fitted to the Sips model, as shown in Fig. 11a. The respective curve for KLT_{MPDET} obtained with non-linear regression is given in Fig. 11b. Complete sets of thermodynamic data for each system studied are listed in Table 4. As observed, cation/basic center interactions for all system are spontaneous in nature as reflected their negative enthalpic values. The series of exothermic enthalpic data did not permit distinguishing a preference of any particular cation to bond with the available basic centers attached to the pendant groups covalently bonded to the inorganic backbone [47,48]. However, the positive entropic values for all interactions that contribute to the favorable interactive process are associated with solvent molecules displacement, initially bonded to the inorganic matrix, which is reinforced by desolvation of the cation before interacting with the

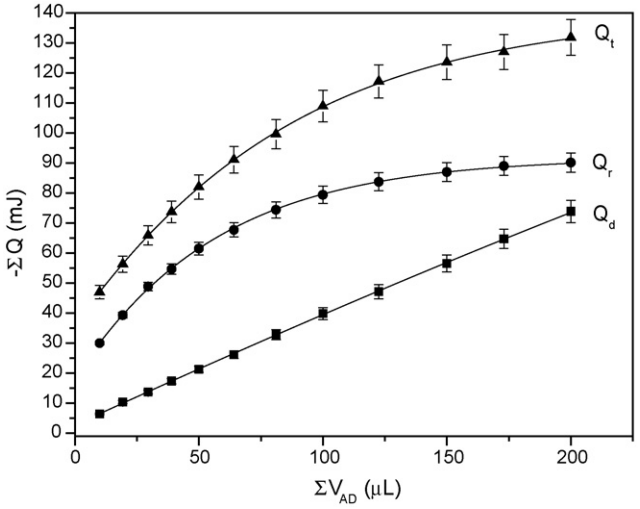

Fig. 12. The resulting thermal effect of adsorption U(VI) on modified kaolinite at 298 ± 1 K. The experiment points represent the thermal effect of cation titration $\sum Q_t$ (▲), cation dilution $\sum Q_d$ (■) and the net thermal effect of interaction $\sum Q_r$ (●), $\sum Q$, and V_{ad} values are the sum of detected thermal effect and total injected volume of U(VI) solution.

Table 4
Thermodynamic data for U(VI) adsorption onto natural and modified kaolinite samples (clay 1.0 g dm^{-3}, pH 4.0, and time 8.0 h).

Sample	N_f^{max} (10^{-3} mmol g^{-1})				N_s (10^{-3} mmol g^{-1})	$-\Delta_{int}h$ (J g^{-1})	$-\Delta_{int}H$ (kJ mol^{-1})	n	$K_S \times 10^{-3}$	$-\Delta_{int}G$ (kJ mol^{-1})	$\Delta_{int}S$ (J K^{-1} mol^{-1})
	298 K	303 K	308 K	313 K							
KLT	8.37 ± 0.11	11.40 ± 0.12	13.36 ± 0.11	15.41 ± 0.10	8.72 ± 0.09	61.05 ± 0.14	7.61 ± 0.11	0.87	6.7 ± 0.1	21.9 ± 0.2	48 ± 1
KLT_{MPDET}	13.87 ± 0.11	15.98 ± 0.10	18.90 ± 0.12	21.91 ± 0.11	13.91 ± 0.11	94.68 ± 0.15	7.27 ± 0.02	0.99	10.4 ± 0.2	22.9 ± 0.1	53 ± 2

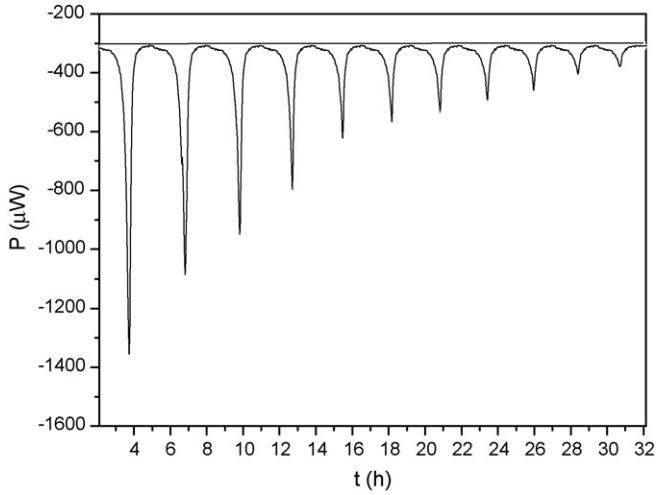

Fig. 13. Variation of the thermal effect versus time upon microcalorimetric titration of unmodified kaolinite (KLT) suspended in water with 20.0 cm^{-3} of uranyl cation at 298 ± 1 K. (clay 3.0 g dm^{-3}, initial U(VI) 25.0 mg dm^{-3}, pH 2.0, and controlled temperature in 298 ± 1 K).

basic centers. In such interactive processes the increase in free molecules in the reaction medium gives a positive entropy, thus demonstrating a favorable set of thermodynamic data for this kind of system [47,48].

The adsorption process was also calorimetrically monitored by titration process. From this value, the thermal effect related to cation-basic center interactions on the modified surface is obtained [48]. An illustration of all the steps of calorimetric titration of 0.020 g of the original kaolinite (KLT) with 2.0×10^{-2} mmol dm^{-3} of U(VI) solution is shown in Fig. 12. This value was adjusted to the modified Langmuir model (Eq. (3)), which is:

$$\frac{\Sigma X}{\Sigma \Delta_r H} = \frac{\Sigma X}{\Delta_{int} H} + \frac{1}{\Delta_{int} H (K_L - 1)} \quad (3)$$

where ΣX is the sum of the mole fraction of each cation in solution, after adsorption, obtained for each experimental point of titrand addition. Δ_rH is the integral enthalpy of adsorption for each point of the calorimetric titration obtained by dividing the thermal effect resulting from adsorption by the number of moles of adsorbate. K_L is the proportionality constant that also includes the equilibrium constant. $\Delta_{int}H$ is the thermal effect of formation of a monolayer on the surface. The thermodynamic cycle for this series of adsorptions involving a suspension (susp) of kaolinite samples (KLT_X) in aqueous (aq) solution with metallic cation (M^{6+}) can be represented by the following calorimetric reactions (Eqs. (4)–(7)):

$$KLT_{X(susp)} + M^{6+}{}_{(aq)} \rightarrow KLT_X{\cdot}M^{6+}{}_{(susp)} \qquad \Sigma Q_t \quad (4)$$

$$KLT_{X(susp)} + nH_2O \rightarrow KLT_X{\cdot}nH_2O \qquad \Sigma Q_h \quad (5)$$

$$M^{6+}{}_{(aq)} + nH_2O \rightarrow M^{6+}{\cdot}nH_2O_{(aq)} \qquad \Sigma Q_d \quad (6)$$

$$KLT_{X(susp)} + M^{6+}{}_{(aq)} \rightarrow KLT_X{\cdot}M^{6+} \qquad \Sigma Q_r \quad (7)$$

Fig. 13 shows as an example, one of the titration thermograms obtained when KLT_{MPDET} adsorbs the U(VI) cation: it shows that, under the conditions applied, equilibrium is attained rapidly. The integrated hest value is obtained by use of the data treatment Digitam 4.1 program (Thermometric).

The Gibbs free energy, entropy and enthalpy values are listed in Table 4. These values suggest that, during complex formation, desolvation disturbs the structure of the reaction medium to promote the disorganization of the system and, consequently, leads to an increase in entropy [24,47,48].

4. Summary

The immobilization of the N-[3-[(trimethoxysilyl)propyl]-diethylenetriamine (MPDET) molecule onto phyllosilicate surface was obtained with success though heterogeneous routes. The adsorption of the metallic ion depended on pH and shaking contact time. The optimum pH for the adsorption of the U(VI) ion ranged from 4.0 to 5.0 for all systems and the minimum sharking contact time necessary for reaching the equilibrium was about 20 and 40 min, for KLT and KLT_{MPDET}, respectively. At $P_{CO_2} = 10^{-3.5}$ atm, uranyl uptake on natural and modified kaolinite surfaces was sensitive to changes in pH and ionic strength. The adsorption maximized at near neutral pH values, and decreased with increasing pH. An increasing in sodium nitrate concentrations from 0.02 to 0.5 mol dm^{-3} resulted in decreasing at pH > 7.5. Through calorimetric investigation information about all systems was obtained, resulting in exothermic enthalpy, negative Gibbs free energy and positive entropy. This series of thermodynamic data reflects the favorable cation/base center interaction at the solid/liquid interface.

Acknowledgements

The authors are indebted to CNPq for fellowships and FAPESP for financial support.

References

[1] R.J. Finch, R.C. Ewing, The corrosion of uraninite under oxidizing conditions, J. Nucl. Mater. 190 (1992) 133–156.
[2] D.J. Wronkiewicz, J.K. Bates, T.J. Gerding, E. Veleckis, B.S. Tani, Uranium release and secondary phase formation during unsaturated testing of UO_2 at 90 °C, J. Nucl. Mater. 190 (1992) 107–127.
[3] D.L. Guerra, A.A. Pinto, C. Airoldi, R.R. Viana, Adsorption of uranyl (II) into modified lamellar Na-Kanemite, Inorg. Chem. Commun. 11 (2008) 539–544.
[4] D.M. Sherman, C.L. Peacock, C.G. Hbbard, Surface complexation of U(VI) on goethite, Geochim. Cosmochim. Acta 72 (2008) 298–310.
[5] T. Arnold, T. Zorn, H. Zänker, G. Bernhard, H. Nitsche, Sorption behavior of U(VI) on phyllite: experimentas and modeling, J. Contam. Hydrol. 47 (2001) 219–231.
[6] F.A. Pavan, I.S. Lima, E.C. Lima, C. Airoldi, Y. Gushikem, Use of ponkan mandarin peels as biosorbent for toxic metals uptake from aqueous solutions, J. Harzard. Mater. 137 (2006) 527–533.
[7] T. Murakami, T. Sato, T. Ohnuki, H. Isobe, Field evidence for uranium nanocrystallization and its implications for uranium transport, Chem. Geol. 221 (2005) 117–126.
[8] D.O. Cooney, Adsorption Design For Wastewater Treatment, Lewis Publishers, Boca Raton, 1999, p. 189.
[9] D.L. Guerra, C. Airoldi, The performance of urea-intercalated and delaminated kaolinite-adsorption kinetics involving copper and lead, J. Braz. Chem. Soc. 20 (2009) 19–30.
[10] T.E. Payne, J.A. Davis, G.R. Lumpkin, R. Chisari, T.D. Waite, Surface complexation model of uranyl sorption on Georgia kaolinite, Appl. Clay Sci. 26 (2004) 151–162.
[11] R.J. Pruett, H.L. Webb, Sampling and analysis of KGa-1B well crystallized kaolin source clay, Clays Clay Miner. 41 (1993) 514–519.
[12] C.A. Coles, R.N. Yong, Aspects of kaolinite characterization and retention of Pb and Cd, Appl. Clay Sci. 22 (2002) 39–45.
[13] B. Lee, Y. Kim, H. Lee, J. Yi, Synthesis of functionalized porous silicas via templating method as heavy metal ion adsorbents: the introduction of surface hydrophilicity onto the surface of adsorbents, Microporous Mesoporous Mater. 50 (2001) 77–90.
[14] X. Pang, F. Tang, Morphological control of mesoporous materials using inexpensive silica sources, Microporous Mesoporous Mater. 85 (2005) 1–6.
[15] J.A.A. Sales, G.C. Petrucelli, F.J.V.E. Oliveira, C. Airoldi, Mesoporous silica originating from a gaseous ammonia epoxide ring opening and the thermodynamic data on some divalent cation adsorption, J. Colloid Interface Sci. 315 (2007) 426–433.
[16] D.L. Guerra, C. Airoldi, K.S. de Sousa, Adsorption and thermodynamic studies of Cu(II) and Zn(II) on organofunctionalized-kaolinite, Appl. Surf. Sci. 254 (2008) 5157–5163.
[17] D.L. Guerra, M.A. Carvalho, V.L. Leidens, A.A. Pinto, R.R. Viana, C. Airoldi, Imobilization of 5-amino-1,3,4-thiazole-thiol onto kanemite for thorium (IV) removal, thermodinamic and equilibrium study, J. Colloid Interface Sci. 338 (2009) 30–39.
[18] R. Sips, On the structure of a catalyst surface, J. Chem. Phys. 16 (1948) 490–495.
[19] E.F.S. Vieira, A.R. Cestari, E.B. Bastos, F. Dias, Interaction of Ag(I), Hg(II), and Cu(II) with 1,2-ethanedithiol immobilized on chitosan: thermochemical data from isothermal calorimetry, J. Colloid Interface Sci. 289 (2005) 42–47.
[20] A.M. Lazarin, C. Airoldi, Thermochemistry of intercalation of *n*-alkylmonoamines into lamellar hydrated barium phenylarsonate, Thermochim. Acta 454 (2007) 43–49.
[21] C.W. Davies, Ion Association, Butterworths, London, 1962, 37-53.
[22] A.L. Herbelin, J.C.Westall, 1999. FITEQL: A computer program for the determination of chemical equilibrium constants from experimental data, Version 4.0. Report 99-01. Oregon State University, Corvallis, Oregon.
[23] W.D. Keller, classification of kaolins exemplified by their textures in scanning electron micrographs, Clays Clay Miner. 26 (1978) 1–20.
[24] J.A.A. Sales, A.G.S. Prado, C. Airoldi, The incorporation of propene-1,3-diamine into silylant epoxide group through homogeneous and heterogeneous routes, Polyhedron 21 (2002) 2647–2651.
[25] H.-J. Im, C.E. Barnes, S. Dai, Z. Xue, Functionalized sol-gels for mercury (II) separation: a comparison of mesoporous materials prepared with and without surfactant templates, Microporous Mesoporous Mater. 70 (2004) 57–62.
[26] A.M. Liu, K. Hidajat, S. Kawi, D.Y. Zhao, A new class of hybrid mesoporous materials with functionalized organic monolayers for selective adsorption of heavy metal ions, Chem. Commun. (2000) 1145–1146.
[27] E.I. Unuabonah, B.I. Olu-Owolabi, K.O. adebowale, A.E. Ofomaja, Adsorption of lead and cadmium ions from aqueous solutions by tripolyphosphate-impregnated kaolinite clay, Colloids Surf., A 292 (2007) 202–211.
[28] W. Stumm, B. Sulzberger, The cycling of iron in nature environments: considerations based on laboratory studies of heterogeneous redox process, Geochim. Cosmochim. Acta 56 (1992) 3233–3257.
[29] J.M. Zachara, J.P. McKinley, Influence of hydrolysis on the sorption of metal-cation by smectites: Importance of edge coordination reactions, Aquat. Sci. 55 (1993) 250–261.
[30] J.M. Zachara, S.C. Smith, C.X. Liu, J.P. McKinley, R.J. Serne, P.L. Gassman, Sorption of Cs^+ to micaceous subsurface sediments from the Hanford site, USA, Geochim. Cosmochim. Acta 66 (2002) 193–211.
[31] R. Guillaumont, T. Fanghanel, V. Neck, J. Fuger, D.A. Palmer, I. Grenthe, M.H. Rand, Update on the Thermodynamics of Uranium, Neptunium, Plutonium, Americium, and Technetium, Elsevier, Amsterdam, 2003.
[32] F.S. Nakayama, Thermodynamic functions for the dissociation of $NaHCO^0$ $NaCO_3^-$, HCO_3^-, and $H_2CO_3^-$, J. Inorg. Nucl. Chem. 33 (1971) 1287–1291.
[33] L.N. Moyes, R.H. Parkman, J.M. Charnock, D.J. Vaughan, F.R. Livens, C.R. Hughes, Uranium uptake from aqueous solution by interaction with goethite, lepdocrocite, muscovite, and mackinawite: an X-ray absorption spectroscopy study, Environ. Sci. Technol. 34 (2000) 1062–1068.
[34] E.R. Sylwester, E.A. Hudson, P.G. Allen, The structure of uranium (VI) sorption complexes on silica, alumina and montmorillonite, Geochim. Cosmochim. Acta 64 (2000) 2431–2438.
[35] A. Tsunashima, G.W. Brindley, M. Bastovanov, Adsorption of uranium from solutions by montmorillonite, compositions and properties of uranyl montmorillonite, Clays Clay Miner. 29 (1981) 10–16.
[36] J.G Catalano, G.E. Brown Jr., Uranyl adsorption onto montmorillonite: evaluation of binding sites and carbonate complexation, Geochim. Cosmochim. Acta 12 (2005) 2995–3005.
[37] Y. Arai, M. McBeath, J.R. Bargar, J. Joye, J.A. Davis, Uranyl adsorption and surface speciation at the imogolite-waster interface: self-consistent spectroscopic and interface complexation models, Geochim. Cosmochim. Acta 70 (2006) 2492–2509.
[38] S.Y. Lee, M.H. Baik, Y.B. Lee, Adsorption of uranyl ions and microscale distribution on Fe-bearing mica, Appl. Clay Sci. 44 (2009) 259–264.
[39] P. Sharma, G. Singh, R. Tomar, Synthesis and characterization of an analogue heulandite: sorption applications for torium (IV), europium (III), samarium (II), and iron (III) recovery from aqueous waster, J. Colloid Interface Sci. 332 (2009) 298–308.
[40] Z. Niu, F. Qiaohui, W. Wenhua, X. Junzheng, C. Lei, W. Wangsuo, Effect of pH, ionic strength and humic acid on the sorption of uranium (VI) to attapulgite, Appl. Radiat. Isot. 67 (2009) 1582–1590.
[41] W. Um, R.J. Serne, C.F. Brown, G.V. Last, U(VI) adsorption on aquifer sediments at the Hanford Site, J. Contam. Hydrol. 93 (2007) 255–269.
[42] Z. Hongxia, X. Yongxin, T. Zuyi, Sorption of uranyl ions gibbsite: effects of contact time, pH, ionic strength, concentration and anion of electrolyte, Colloids Surf., A 252 (2005) 1–5.
[43] G. Redden, J. Bargar, R. Brenchikh-Latmani, Citrate enhanced uranyl adsorption on goethite: An EXAFS analysis, J. Colloid Interface Sci. 244 (2001), 221-219.
[44] P. Sharma, R. Tomar, Synthesis and application of an analogue of mesolite for removal of uranium (VI), thorium (IV), and europium (III) from aqueous waste, Microporous Mesoporous Mater. 116 (2008) 641–652.
[45] X. Tang, Z. Li, Y. Chen, Adsorption behavior of Zn(II) on calcinated Chinese loess, J. Harzard. Mater. 161 (2009) 824–834.
[46] T.R. Macedo, G.C. Petrucelli, C. Airoldi, Silicic acid magadiite guest molecules and features related to the thermodynamics of intercalation, Clays Clay Miner. 55 (2007) 151–159.
[47] R. Dey, C. Airoldi, Designed pendant chain covalently bonded to silica gel for cation removal, J. Hazard. Mater. 156 (2008) 95–101.
[48] I.S. Lima, C. Airoldi, A thermodynamic investigation on chitosan-divalent cation interactions, Thermochim. Acta 421 (2004) 133–139.